The plasma membrane Ca²⁺ pump PMCA4b inhibits the migratory and metastatic activity of BRAF mutant melanoma cells

Hegedus, L.[1], Garay, T.[2,3], Molnar, E.[2], Varga, K.[2], Bilecz A.[2], Torok, S.[4], Padanyi, R.[2], Paszty, K.[5], Wolf, M[6], Grusch, M.[6], Kallay, E.[1], Dome, B.[4,7,8,9], Berger, W.[6], Hegedus, B.[7,10,11], Enyedi, A.[2,11]

[1]Department of Pathophysiology and Allergy Research, Comprehensive Cancer Center Vienna, Medical University of Vienna
[2]2nd Institute of Pathology, Semmelweis University, Budapest
[3]Department of Biological Physics, Eötvös University, Budapest
[4]National Koranyi Institute of Pulmonology, Budapest, Hungary
[5]Molecular Biophysics Research Group of the Hungarian Academy of Sciences and Department of Biophysics, Semmelweis University, Budapest, Hungary
[6]Institute of Cancer Research, Department of Medicine I, Comprehensive Cancer Center Vienna, Medical University of Vienna
[7]Division of Thoracic Surgery, Department of Surgery, Comprehensive Cancer Center, Medical University of Vienna
[8]Department of Thoracic Surgery, National Institute of Oncology-Semmelweis University, Budapest
[9]Department of Biomedical Imaging and Image-guided Therapy, Medical University of Vienna, Austria
[10]Department of Thoracic Surgery, Ruhrlandklinik, University Clinic Essen, Essen, Germany
[11]Molecular Oncology Research Group of the Hungarian Academy of Sciences and Semmelweis University, Budapest, Hungary

Running Title: Anti-metastatic activity of PMCA4b

Keywords: PMCA4b, BRAF mutant melanoma, migration, metastasis

Abbreviations used:

PMCA4b: plasma membrane Ca^{2+} ATPase isoform 4b
ORAI1: Orai calcium release-activated calcium modulator 1
SERCA: sarco/endoplasmic reticulum Ca^{2+} ATPase
SOCE: store-operated Ca^{2+} entry
STIM1: stromal interaction molecule 1
IP3R: inositol 1,4,5-triphosphate receptor
RYR2: ryanodine receptor 2
TRPM1: transient receptor potential cation channel subfamily M member 1
NFAT: nuclear factor of activated T-cells
HUVEC: human umbilical vein endothelial cell

Novelty and Impact: This study reveals a crosstalk between Ca^{2+} signaling and oncogenic activation of the MAPK pathway through the regulation of PMCA4b expression. This is the first study to show that PMCA4b inhibits migration of BRAF mutant melanoma cells without affecting their proliferation and propose that PMCA4b is a previously unrecognized metastasis suppressor protein in melanoma.

Corresponding Authors: Agnes Enyedi, Molecular Oncology Research Group of the Hungarian Academy of Sciences and 2nd Institute of Pathology, Semmelweis University, Budapest Hungary; Phone/ Fax: +3612156921 Email: enyedi.agnes@med.semmelweis-univ.hu; Balázs Hegedűs, Department of Thoracic Surgery, Ruhrlandklinik, University Clinic Essen, Essen, Germany and Molecular Oncology Research Group of the Hungarian Academy of Sciences and Semmelweis University, Budapest, Hungary; Phone/Fax: +3612156921 Email: balazs.hegedus@meduniwien.ac.at

Abstract

Oncogenic mutations of BRAF lead to constitutive ERK activity that supports melanoma cell growth and survival. While Ca^{2+} signaling is a well-known regulator of tumor progression, the crosstalk between Ca^{2+} signaling and the Ras-BRAF-MEK-ERK pathway is much less explored. Here we show that in BRAF mutant melanoma cells the abundance of the plasma membrane Ca^{2+} ATPase isoform 4b (PMCA4b, ATP2B4) is low at baseline but markedly elevated by treatment with the mutant BRAF specific inhibitor vemurafenib. In line with these findings gene expression microarray data also shows decreased PMCA4b expression in cutaneous melanoma when compared to benign nevi. The MEK inhibitor selumetinib – similarly to that of the BRAF-specific inhibitor - also increases PMCA4b levels in both BRAF and NRAS mutant melanoma cells suggesting that the MAPK pathway is involved in the regulation of PMCA4b expression. The increased abundance of PMCA4b in the plasma membrane enhances $[Ca^{2+}]_i$ clearance from cells after Ca^{2+} entry. Moreover we show that both vemurafenib treatment and PMCA4b overexpression induce marked inhibition of migration of BRAF mutant melanoma cells. Importantly, reduced migration of PMCA4b expressing BRAF mutant cells is associated with a marked decrease in their metastatic potential *in vivo*. Taken together, our data reveal an important crosstalk between Ca^{2+} signaling and the MAPK pathway through the regulation of PMCA4b expression and suggest that PMCA4b is a previously unrecognized metastasis suppressor.

Introduction

Malignant melanoma is a highly invasive and metastatic type of cancer with poor prognosis. In melanoma BRAF is the most frequently mutated oncogene - present in up to 60% of tumors - that induces the constitutive activation of the RAS-RAF-MEK-ERK signaling cascade [1, 2]. The introduction of vemurafenib – an inhibitor showing considerable selectivity towards the predominant V600E mutant form of BRAF – fundamentally changed the therapeutic options for melanoma [3, 4]. Nevertheless, a number of BRAF mutant melanomas show limited response due to intrinsic resistance and initially responding patients often relapse due to acquired resistance [5, 6]. Although recent advances in immunotherapy have led to important improvements in clinical outcome, monotherapy is often insufficient for melanoma treatment [7]. Therefore, further studies are needed to identify additional molecular targets to fight this malignancy more effectively.

Cell migration is a prerequisite for invasion that consequently contributes to tumor progression and metastasis [8]. Ca^{2+} signaling regulates several steps in the migratory process, such as relocation of focal adhesions, rear-end retraction and cytoskeleton redistribution [9]. It has been shown in several types of cancer that specific mutations and/or changes in subcellular localization of certain Ca^{2+} transporting molecules can significantly alter intracellular Ca^{2+} signaling [10, 11]. The expression of Ca^{2+} channels RyR2 and P2X7 was found to be upregulated in BRAF mutant melanoma cells; and P2X7 was shown to have an antiapoptotic effect upon simultaneous stimulation with apoptosis inducer 2ME (2-methoxyestradiol) and P2X7 agonist ATP. Conversely, downregulation of P2X7 expression by siRNA sensitized the cells to 2ME treatment [12]. Increased Ca^{2+} influx through store operated Ca^{2+} entry was shown to promote the migratory and metastatic activity of melanoma cells [13, 14]. Furthermore, stromal interaction molecule 1 (STIM1) and Orai calcium release-activated calcium modulator 1 (ORAI1) initiated Ca^{2+}

oscillations that were found to promote invadopodium assembly and extracellular matrix (ECM) degradation in melanoma cells [15]. Silencing of ORAI and STIM proteins decreased migratory and metastatic potential of melanoma cells [13-15]. Additionally, T-type channel blockers of clinical use (mibefradil and pimozide) reduced the proliferation rate and promoted cell death in a metastatic melanoma cell line [16]. It was also shown that combined treatment of vemurafenib with thapsigargin – an inhibitor of the sarco/endoplasmic reticulum Ca^{2+} ATPase (SERCA) and an endoplasmic reticulum (ER) stress inducer - could induce apoptosis even in vemurafenib resistant cells [17].

The Ca^{2+} extrusion proteins in the plasma membrane, the plasma membrane Ca^{2+} ATPases (PMCAs), are critical regulators of the maintenance of cellular Ca^{2+} homeostasis and thus regulate vital cellular processes such as cell cycle, apoptosis or migration [18]. These pumps are encoded by four different genes (PMCA1-4), and alternative mRNA splicing results in more than 20 variants [19]. Changes in PMCA expression during malignant transformation have been described in several tumor types, but not in melanoma so far. Major alterations were identified in the expression and activity of certain PMCA isoforms in colorectal [20, 21] and breast cancer cells [22, 23]. PMCA4 expression was down-regulated in colorectal tumor tissues as compared to normal colon tissue [24].

In this study, we investigated the role of PMCAs in the maintenance of intracellular Ca^{2+} homeostasis in melanoma cells. We show that in BRAF mutant melanoma cells, vemurafenib treatment strongly increased the abundance of PMCA4b in the plasma membrane and enhanced $[Ca^{2+}]_i$ clearance after stimulation. We also demonstrated that both vemurafenib treatment and PMCA4b overexpression inhibited the migration of BRAF mutant melanoma cells. Furthermore,

we provide in vivo evidence that PMCA4b overexpression decreased the metastatic activity of BRAF-mutant melanoma cells.

Material and methods

Cell culture: Two BRAF(V600E) mutant (A375, A2058,), an NRAS mutant (MJZJ (VM15)) and two BRAF/NRAS wild-type (MEWO,) melanoma cell lines were used. MEWO, A375 and A2058 were purchased from ATCC. MJZJ cell line was established at the Institute of Cancer Research at the Medical University of Vienna [25]. All cell lines including the genetically modified A375 cells were subjected to STR analysis at the Medical University of Vienna. Cells were cultured in DMEM supplemented with 10% FBS, 100 mg/ml streptomycin, 100 U/ml penicillin at $37^{o}C$ and 5% CO_2 in a humidified atmosphere.

Treatment of melanoma cell lines: The BRAF (V600E) specific inhibitors vemurafenib (PLX4032) and GDC0879, and the MEK kinase inhibitor selumetinib (Selleck Chemicals, Munich, Germany) were dissolved in DMSO and stored at $-80^{o}C$. Cells were seeded $1-2x10^{5}$ cells/well in 6-well plates for Western Blot and $1-2x10^{4}$ cells/well in an Imaging Chamber CG 8 Well (PAA) for immunofluorescence staining and Ca^{2+} signal measurements. After 24 hours, fresh medium was added together with the appropriate drug. The final DMSO concentration did not exceed 0.01% in the experiments.

Western Blot Analysis was performed as described previously [21]. Total protein from the cells was precipitated by addition of 6% TCA and was analyzed by Western blot as described previously [21]. The following primary antibodies were used: mouse monoclonal anti-PMCA4b (JA3, dilution 1:1000 The JA3 antibody recognizes the region between residues 1156-1180, which is specific to hPMCA4b [26]. Rabbit polyclonal anti-PMCA1 (Affinity BioReagents, PA1-914, dilution 1:1000),

mouse monoclonal anti-SERCA2 (IID8, dilution 1:2500, Sigma-Aldrich, S1439), mouse monoclonal anti-SERCA3 (PL/IM430, dilution 1:200) described in Ref. [21], rabbit monoclonal anti-phospho-p44/42MAPK (ERK1/2) (Cell Signaling, CST4370S, dilution 1:1000), mouse monoclonal anti-ERK1/2 (MK1) (Santa Cruz, sc135900, dilution:), rabbit polyclonal anti-beta-tubulin (Abcam, ab6046), mouse monoclonal anti-BRAF-V600E (VE$_1$) (Spring Bioscience Corp. E19290),. Subsequently HRP-conjugated anti-rabbit and anti-mouse secondary antibodies (Jackson ImmunoResearch) were applied and for detection Pierce ECL Western Blotting Substrate (Thermo Scientific) and luminography were used. Densitometric analysis was done by ImageJ software v1.42q.

Immunofluorescence: Cells were treated with 0.5 µM vemurafenib for 48 to 72 hours. Cells were washed twice with 37°C PBS and fixed with 4% paraformaldehyde for 15 min at room temperature. Immunostaining experiments using mouse monoclonal anti-PMCA4b antibod JA3 [26], (dilution: 1:200) was performed as described previously [23]. Images were taken by an Olympus IX-81 and a Zeiss LSM500 confocal laser scanning microscopes.

Ca^{2+} *signal measurements*: Cells were treated with 0.5µM vemurafenib for 48/72 hours. Prior to the experiment medium was changed to phenol red-free DMEM containing 10 mM Hepes pH 7.4 and 10% FBS. To measure intracellular Ca^{2+} level we used Fluo-4, AM (Molecular Probes, F14201) green fluorescent Ca^{2+} indicator. Cells were washed twice with HBSS supplemented with 2 mM CaCl$_2$, 0.9 mM MgCl$_2$ and 20 mM HEPES pH7.4, then incubated with 0.5 µM Fluo-4 AM for 30 min at RT. Then cells were again washed twice and medium was changed to nominally Ca^{2+} free HBSS supplemented with 100 µM EGTA, 100 µM CaCl$_2$, 0.9 mM MgCl$_2$ and 20 mM HEPES pH 7.4. First we depleted the internal Ca^{2+} stores by adding 2 µM thapsigargin and 2 minutes later 100 µM ATP. After an additional 3 minutes the external Ca^{2+}

level was restored to 2 mM with the addition of $CaCl_2$. Ca^{2+} influx through store operated Ca^{2+} channels was followed for an additional 15 minutes. Ca^{2+} signals were also induced by A23187. After the medium was replaced by HBSS supplemented with 0.9 mM $MgCl_2$, 2 mM $CaCl_2$ and 20 mM HEPES pH 7.4, Ca^{2+} influx was triggered by the addition of 2 μM A23187. In order to inhibit PMCA activity, 1mM $LaCl_3$ was added at the A23187-induced peak Ca^{2+}. Images were taken by Olympus IX-81 confocal laser scanning microscope with a 60x (1.4) oil immersion objective and Fluoview FV500 software v4.1. Z-resolution was set to 1 μm, images were taken every 0.3 s. The relative fluorescence intensities were calculated as F/F_o (where F_o was the average initial fluorescence) and data were analyzed with the Prism4 software v4.01 (GraphPad Software).

Migration assay: Cell migration was quantified by videomicroscopic measurements as described earlier [27-29]. Briefly, cells were seeded in the inner 8 wells of 24-well plates (Corning Incorporated, Corning, NY). Following overnight culture in normal medium, the culture medium was changed to CO_2-independent medium (Gibco-BRL Life Technologies, Carlsbad, CA) supplemented with FCS and 4 mM glutamine. Cell movement was recorded in a custom designed incubator built around an inverted phase-contrast microscope (World Precision Instruments, Sarasota, FL) at 37°C and room ambient atmosphere. Images of 3 neighboring microscopic fields in each well were taken every 5 minutes. In case of treatments, after 24 hours of baseline recording, cells were treated with 0.5 μM vemurafenib and images were taken for 72 hours. Migration data were retrieved by a custom made cell-tracking program that enables manual marking of individual cells. Cell motility was quantified as the net displacement of tracked cells between 0-12 and 48-60 hours of recordings with or without treatment using the 15-minute interval images.

Morphological analysis: Image analysis was performed on the videomicroscopic images of A375 cells expressing GFP or GFP-PMCA4b. Computer-based analysis of the morphology of individual cells was performed with ImageJ 1.47v using the Analyze Particle function. Morphological parameters included: cellular area, aspect ratio (defined as (major axis) / (minor axis) of the ellipse which best fits the shape of the cell) and circularity (defined as $4\pi*$ (cell area) / (cell perimeter)^2).

Generation of cell lines: To establish MEWO-GFP, MEWO-GFP-PMCA4b, A375-GFP, A375-GFP-PMCA4b-I and GFP-PMCA4b–II cell lines, the SB-CAG-GFP-PMCA4b-CAG-Puromycin construct was generated which contains a Sleeping Beauty transposon system. The original SB-CAG-GFP-ABCG2-CAG-Puromycin vector was a generous gift from T. Orban [30]. From this vector, GFP-ABCG2 was excised by the AgeI and BclI enzyme pair. Next, GFP-tagged PMCA4b was cut out from the pEGFP-PMCA4b template plasmid [31] in two steps; the vector was opened by a full digestion with ClaI restriction enzyme, then the GFP-PMCA4b was cut out by a partial digest with AgeI and BamHI, and ligated. Stable transfection was performed as described earlier [23, 32]. 2-3.5x10^5 MEWO and A375 cells/well were seeded on a 6-well plate. Cells were transfected with a mixture of SB-CAG-GFP-PMCA4b-CAG-Puromycin transposon construct and SB100x transposase plasmid in a 1:10 ratio using the Fugene HD transfection reagent (Roche Applied Science). 48 hours after transfection, the medium was changed to selection medium containing 1µg/ml puromycin dihydrocloride. Selection was continued until all non-transfected cells had died.

Cell proliferation: Proliferation was measured by ELISA detection of BrdU incorporation (Roche Applied Science, Vienna, Austria, 11 647 229 001) according to the manufacturer's protocol. A375-GFP, A375-PMCA4bI and II cells were seeded in 96-well plates in triplicates (1x10^4

cells/well). 48 hours later cells were labeled with 10 µM BrdU for 2 hours at $37^{o}C$. Absorbance was measured at 370 nm (reference: 492 nm) and calculated as A_{370}-A_{492}.

Quantitative real-time reverse transcription PCR (qPCR): In order to compare the mRNA level of several Ca^{2+} channels and EMT markers mRNA was isolated with TRIzol reagent (Life Technologies) from vemurafenib-treated and control A375 and A2058 cells. Reverse transcription was performed with RevertAid Reverse Transcriptase (Thermo Scientific) and amplification was done with the Maxima SYBR Green maser mix (Thermo Scientific) on an Applied Biosystems® 7500 Real-Time PCR System. Primer pairs for E-cadherin, ZEB1, snail, vimentin and GAPDH (for normalization) were used as previously described [33]. All other primers used are found in Supplementary Table 1. For quantification of PMCA4b transcripts, the TaqMan assays Hs00608066_m1 (PMCA4b) and Hs99999905_m1 (GAPDH, both from Thermo Scientific) were used.

Lung colonization assay: SCID mice were obtained from the National Institute of Oncology, Hungary. A375-GFP, A375-PMCA4bI and II cells were injected ($4x10^5$cells/0.2 ml serum free DMEM) into the tail veins of 11-week old female SCID mice (10 mice / group). 6 weeks after injection, mice were sacrificed and their lungs and the tumor tissue found in the chest cavity were removed. Formalin-fixed and paraffin-embedded (FFPE) tissue blocks were prepared from all lung and tumor tissue samples for each animal and sections were stained with hematoxylin-eosin. Slides were scanned with the TissueFAXS System (TissueGnostics GmbH, Vienna, Austria) (20x) and analyzed with the Tissue Quest program [34]. Tumor regions were marked and their area was quantified. The animal-model protocol was carried out in accordance with the Guidelines for Animal Experiments and were approved for the Department of Experimental Pharmacology in the National Institute of Oncology, Budapest, Hungary (permission number: 22.1/722/3/2010).

Results

PMCA4b is upregulated in BRAF mutant melanoma cells after inhibition of the BRAF-MEK-ERK pathway

Vemurafenib (PLX4032) and GDC0879 are low molecular weight inhibitors targeting mutant BRAF. They block MEK and ERK signaling selectively in cells with a $BRAF^{V600E}$ mutation [35]. Since the expression of plasma membrane Ca^{2+} ATPases are often altered in cancer [20, 21], we tested if treatment of BRAF mutant and wild type melanoma cells with these BRAF specific inhibitors would affect their expression pattern. We treated two BRAF wild type (MEWO, MJZJ) and two BRAF mutant (A375, A2058) melanoma cell lines with vemurafenib (0.5μM) and GDC0879 (0.5μM), and determined the level of PMCA proteins by Western blot analysis (Fig. 1A 1and 1A2). Using isoform-specific anti-PMCA antibodies, we identified PMCA1 and PMCA4b proteins in these cells. While the protein level of PMCA1 was not modified by the treatment in any of the cell lines tested, the level of PMCA4b increased exclusively in the BRAF mutant cell lines. Semi-quantitative densitometric analysis of the Western blots revealed a 4-10 fold increase in the protein level of PMCA4b in these cells (Fig. 1A2, bar graphs). Figures 1B1 and 1B2 show PMCA4b protein level changes in A375 cells treated with increasing concentrations of vemurafenib. Marked upregulation of PMCA4b was seen at the 0.5 μM vemurafenib concentration. Therefore, in further experiments, we treated the cells with 0.5 μM vemurafenib to reach maximal PMCA4b upregulation.

The sarco/endoplasmic reticulum Ca^{2+} ATPases (SERCAs) also play a major role in maintaining intracellular Ca^{2+} homeostasis. Accordingly, we examined the changes in SERCA2 and SERCA3 protein levels in vemurafenib treated A375 cells (Fig. 1B1) and found that only SERCA2 was present in this melanoma cell line, and its protein level was not modified by the treatment.

We also tested the effect of vemurafenib treatment on the mRNA expression of PMCA4b in the A375 BRAF mutant cell line (Supplementary Fig. S1) and found that vemurafenib greatly enhanced the mRNA expression of PMCA4b (a time-course is shown in Supplementary Fig. S1A). We also examined the expression of a number of Ca^{2+} channels and found that vemurafenib treatment did not affect that of the inositol 1,4,5-triphosphate receptor type 1-3 (IP3R1, IP3R2, IP3R3), ORAI calcium release-activated calcium modulator 1 (ORAI1), ryanodine receptor 2 (RYR2) and stromal interaction molecule 1 and 2 (STIM1, STIM2) (Supplementary Fig. S1B) in both BRAF mutant cell lines. The mRNA level of transient receptor potential cation channel subfamily M member 1 (TRPM1) was strongly increased in A2058 cells by the treatment while its amount was negligible in A375 cells even after vemurafenib treatment. These results underline the selectivity of PMCA4b upregulation among the Ca^{2+} signaling molecules in response to BRAF inhibition.

MEK1 and MEK2 enzymes lie downstream of BRAF and upstream of ERK1/2 in the Ras/Raf/MEK/ERK signal transduction pathway [36] therefore we treated BRAF mutant melanoma cell lines (A375, A2058) with selumetinib (AZD6244) (0.5µM), a highly selective MEK1/2 inhibitor [37]. We found that it upregulated PMCA4b to a similar extent as the BRAF selective inhibitor, vemurafenib (Fig. 1C1 and 1C2). Furthermore, selumetinib treatment enhanced PMCA4b protein level not only in the BRAF mutant cells but also in an NRAS mutant cell line (MJZJ) suggesting that the BRAF/MEK signaling pathway has a key function in the altered protein level of PMCA4b. The relative amount of PMCA4b protein increased 3-5 fold upon selumetinib treatment in both cell types (Fig. 1C2).

Increased plasma membrane abundance of PMCA4b in vemurafenib-treated BRAF mutant cells is associated with enhanced Ca^{2+} clearance

Confocal microscopy analysis demonstrated that vemurafenib treatment substantially increased the level of PMCA4b protein in the plasma membrane of BRAF-mutant melanoma cells (Fig. 2A). To study how changes in PMCA4b abundance affected Ca^{2+} signaling in these cells, we performed Ca^{2+} signal measurements by confocal imaging. In order to induce store-operated Ca^{2+} entry (SOCE), the extracellular Ca^{2+} concentration was restored to 2 mM free Ca^{2+} after the intracellular Ca^{2+} stores were depleted in nominally zero Ca^{2+} environment[38]. In vemurafenib-treated BRAF mutant cells, intracellular Ca^{2+} concentration declined to basal level clearly faster after the SOCE peak than in the untreated cells, whereas vemurafenib had no effect on Ca^{2+} clearance in BRAF wild type cells (Fig. 2B,C1,2 and Supplementary Fig. S2). Similar results were obtained when the Ca^{2+} signal was initiated independently of the Ca^{2+} entry machinery using the Ca^{2+} ionophore, A23187 (Fig. 2D1,2,3 and Supplementary Fig. S2A). To further verify the role of PMCA in Ca^{2+} clearance, we used lanthanum which is a well-known inhibitor of PMCAs. In order to avoid altering the Ca^{2+} entry pathways we added $LaCl_3$ immediately after the ionophore induced Ca^{2+} peak and found that lanthanum strongly inhibited the decay phase of the transient (Fig. 2D1,2). These results indicate that the up-regulated PMCA4b in BRAF mutant cells was fully functional and it was mostly responsible for the faster Ca^{2+} clearance after stimulation.

Vemurafenib inhibits the migration of BRAF mutant melanoma cells

Activation of the BRAF/MEK/ERK pathway changes the expression of several proteins involved in the migratory process [39, 40]. Therefore, we examined the effect of vemurafenib treatment on the migratory activity of a BRAF wild type (MEWO) and two different BRAF mutant melanoma cell lines (A2058, A375) (Figure 3). The migration of the cells was recorded by time-lapse video microscopy for 72 hours. Representative trajectories of single cells after 48 hours of vemurafenib

treatment clearly show that vemurafenib slows down the migration of the BRAF mutant A375 cell line (Figure 3A). The graphs in Figure 3B show that the inhibition of migratory activity of BRAF mutant cells was more pronounced after treating the cells for 48 hours (48-60 hours) while short (0-12 hours) exposure to the drug did not reduce (A2058) or only slightly (A375) decreased cell migration. The rate of inhibition coincided with the vemurafenib-induced increase in PMCA4b abundance that reached saturation at 48-72 hours after exposure to the drug (Supplementary Fig. S1A). BRAF wild type cells (MEWO) migrated much slower than the BRAF mutant cells and their migratory activity did not change in response to vemurafenib treatment, as expected (Fig. 3B).

PMCA4b overexpression decreases the migratory activity of BRAF mutant A375 cells

The role of store operated Ca^{2+} entry (SOCE) in melanoma migration has been proposed, but the role of Ca^{2+} extrusion molecules such as the PMCA has not been addressed in this respect [13, 14]. Since vemurafenib markedly enhanced the abundance of PMCA4b in the plasma membrane and decreased cell migration, we investigated how overexpression of the PMCA4b protein affected melanoma cell motility. To address this we stably transfected MEWO (BRAF wild type) and A375 (BRAF mutant) cell lines with GFP (control) and GFP-PMCA4b (Fig. 4A, B). Western blot analysis showed that the newly introduced GFP-PMCA4b protein was expressed in the physiological range both in the two independently generated PMCA4b overexpressing A375 (GFP-PMCA4b-I and GFP-PMCA4b-II; Fig. 4A) and the BRAF wild type MEWO cell lines. Confocal imaging demonstrated that the overexpressed pump localized mostly in the plasma membrane (Fig. 4B). Next we examined whether PMCA4b overexpression affects the proliferation of the BRAF-mutant cells using the BrdU incorporation assay. While 48-hour vemurafenib treatment strongly decreased proliferation, there were no significant differences

14

between control and PMCA4b overexpressing A375 cells (Fig. 4C).We also showed that the expression levels of BRAFV600E, pERK and the Ca^{2+} pump of the internal Ca^{2+} stores SERCA2 were not altered by PMCA4b overexpression (Fig. 4A, Supplementary Fig. S3A).

Next we compared cell motility of A375-GFP and A375-GFP-PMCA4b cell lines and found that PMCA4b strongly decreased the migratory activity of A375 cells (Fig. 5A1,2 and Supplementary Movies S1 and S2). Similarly to the vemurafenib-treated control cells, GFP-PMCA4b overexpressing A375 cells migrated significantly shorter distances in the given time frame than the untreated GFP-expressing A375 cells (Fig. 5A1,2).

Changes in motility can be correlated with alterations in cytoskeletal and morphology properties of cells [41]. Remarkably, the reduced migratory activity of GFP-PMCA4b BRAF mutant cells associated with a profoundly altered cell shape. Figure 5B1 show that the GFP-PMCA4b expressing cells are more round, with a typical front-to-rear polarity, in contrast to the slender shape of GFP expressing control cells showing more outgrowth that also changes frequently during migration (compare Supplementary Movies 1 and 2). Significant differences were found among the morphological parameters of the different types of cells; PMCA4b expressing cells showed significantly larger area and circularity, and smaller aspect ratio than control A375 cells (Fig. 5B2, bar graphs).

Because of this change in morphology, we analyzed the expression of certain EMT marker proteins, such as E-cadherin, ZEB1, Snail and vimentin [42] by real-time quantitative PCR but no difference in their mRNA expression was found between control and PMCA4b overexpressing A375 cells. Of note, there was no detectable E-cadherin expression in the A375 cells with or without GFP-PMCA4b either (Supplementary Fig. S3B).

Altogether, these data demonstrate that overexpression of PMCA4b changes morphology and reduces migratory activity of BRAF mutant A375 cells without having any significant anti-proliferative effect. It is important to note that selective inhibition of BRAF by vemurafenib inhibits both proliferation and migratory activity of these cells.

PMCA4b overexpression decreases the metastatic activity of BRAF mutant A375 cells in vivo

Since migration is a key step in metastasis formation, we compared the metastatic activity of A375-GFP and A375-GFP-PMCA4b cell lines *in vivo* by performing a lung colonization assay. 6 weeks after tail vein injection, the number of animals with lung metastasis was significantly lower in the groups injected with PMCA4b overexpressing A375 cells as compared with controls (Fig. 6A). The total area of tumors was dramatically reduced in mice injected with the A375-GFP-PMCA4b cells than in the control group (Fig. 6B), as representative pictures of cross sections of lungs from A375-GFP-, A375-GFP-PMCA4b-I- and A375-GFP-PMCA4b-II-injected mice show. Of note, control A375 cells could establish tumors in the lung parenchyma and smaller groups of tumor cells invaded the normal lung tissue along blood vessels or bronchioles in five out of the 8 tumor bearing mice. In contrast, A375-GFP-PMCA4b-I and -II cells formed smaller tumors and their majority was growing on the surface or in the connective tissue compartment of the lungs. Five out of the six tumor-bearing mice injected with A375-GFP-PMCA4b-I or -II cells showed no sign of invasion of the lung parenchyma. This is the first demonstration that PMCA4b has the ability to reduce the metastatic potential of a BRAF-mutant melanoma cell line.

In order to demonstrate that PMCA4 expression is related to the malignant progression of melanoma, we analyzed two datasets in the ONCOMINE database [43] where benign nevi and

melanoma specimens could be directly compared (Suppl. Fig. 4). In both datasets the proportion

of cases with high PMCA4 expression was higher in benign nevi than in melanoma cases [44, 45].

Pooling the data from the two cohorts, 21 out of 27 (77%) benign nevi had high PMCA4

expression in contrast to 26 out of 69 (38%) melanomas.

Discussion

In this paper we describe for the first time that a particular variant of the plasma membrane Ca^{2+}

transport ATPase, PMCA4b, regulates cell motility and metastatic capacity of BRAF mutant

melanoma cells. We showed that PMCA4b is upregulated upon inhibition of mutant BRAF.

Further, we demonstrated that both vemurafenib treatment and PMCA4b overexpression

inhibited migration of BRAF mutant cells and the reduced motility of PMCA4b expressing cells

was accompanied by a profound change in cell shape. Moreover, we found that overexpression of

PMCA4b suppressed metastatic activity of the invasive BRAF mutant A375 cell line. While

PMCA4b inhibited motility and metastatic activity of BRAF mutant cells, it did not affect cell

growth which by definition is a characteristic of metastasis suppressor genes [46, 47].

It has been suggested that enhanced Ca^{2+} signaling through store-operated Ca^{2+} entry can increase

cell motility and metastasis. Increased expression of STIM and ORAI proteins caused increased

migratory activity of breast cancer [48], rat aortic vascular smooth muscle [49] and melanoma cells [50, 51]. Inhibition of SOCE by knockdown of STIM and ORAI proteins caused a marked decrease in

the migratory and metastatic potential of tumor cells. In good accordance with these findings the

down-regulation of cGMP-specific phosphodiesterase PDE5A induced elevated cytosolic Ca^{2+}

levels specifically in BRAF mutant melanomas that resulted in increased contractility and

induction of invasion [52]. We may hypothesize that down-regulation of PMCA4b expression also

contributes to the elevated cytosolic Ca^{2+} levels and enhanced cell motility of malignant cells. In our study we demonstrated that in BRAF mutant cells PMCA4b enhanced cytosolic Ca^{2+} clearance induced either through the activation of the store operated channels or by the ionophore, A23187. We showed previously that PMCAs can influence the pattern of SOCE mediated Ca^{2+} signals [38]. These findings support the notion that PMCA4b decreases the migratory activity of melanoma cells at least partially through opposing the SOCE mediated Ca^{2+} signal. This is supported by the fact that the expression level of store operated Ca^{2+} channels (ORAI1, STIM1 and 2) and inositol 1,4,5-triphosphate receptors type 1-3 (IP3R1, IP3R2, IP3R3) were not altered by vemurafenib treatment.

Our data is in line with other recent observations on endothelial cell migration. It has been shown that PMCA4 localizes mostly at the cell front of migrating human umbilical vein endothelial (HUVEC) cells and that it is essential in maintaining the Ca^{2+} gradient necessary for directed cell migration [53]. Another group demonstrated that PMCA4 inhibited the motility of VEGF-activated endothelial cells through its inhibitory effect on the calcineurin/NFAT pathway [54]. This is the first time, however, to show that PMCA4b changes shape and motility of a highly aggressive tumor cell line.

Identification of metastasis suppressor genes is of utmost importance since more than 90 % of cancer patients die from metastasis. Our findings suggest that PMCA4b is a major regulator of cell migration and thus of metastatic potential in an exceedingly metastatic malignancy. We found that both mutant BRAF and MEK inhibitor treatment increased PMCA4b abundance in malignant melanoma cells. Furthermore, there were a significantly lower number of cutaneous melanoma cases with high PMCA4b expression when compared to benign nevi in two gene expression microarray datasets available through the ONCOMINE database. These finding

further supports the association of malignant progression with the decrease of PMCA4b expression in melanoma.

In summary, here we demonstrate for the first time that PMCA4b is a metastatic suppressor protein. We discovered that enhanced PMCA4b abundance induced significant changes in cell shape and motility of a BRAF mutant cell line without affecting proliferation. The pronounced change in cell shape and motility suggest that PMCA4b expression can alter actin polymerization dynamics in highly metastatic cell types and hence inhibit metastasis. Our data support the idea that the enhanced Ca^{2+} clearance contributes to the anti-metastatic function of the pump.

Acknowledgement

Authors' contributions

LH, BH and AE conceived and designed experiments, LH, KV, TG and KP developed methodology. LH, TG, MW, ST, EM, AB, SK and BD carried out experiments, LH, AE, RP and BH analyzed and interpreted the data. LH, AE, BH, EK, MG and WB were involved in writing

the paper. AE supervised the study. All authors had final approval of the submitted and published versions.

Conflict of Interest: No potential conflicts of interest were disclosed.

References

1. Pratilas CA, Xing F, Solit DB. Targeting oncogenic BRAF in human cancer. *Curr Top Microbiol Immunol* 2012;**355**: 83-98.

2. Houben R, Becker JC, Kappel A, Terheyden P, Brocker EB, Goetz R, Rapp UR. Constitutive activation of the Ras-Raf signaling pathway in metastatic melanoma is associated with poor prognosis. *J Carcinog* 2004;**3**: 6.

3. Ascierto PA, Kirkwood JM, Grob JJ, Simeone E, Grimaldi AM, Maio M, Palmieri G, Testori A, Marincola FM, Mozzillo N. The role of BRAF V600 mutation in melanoma. *Journal of translational medicine* 2012;**10**: 85.

4. Huang T, Karsy M, Zhuge J, Zhong M, Liu D. B-Raf and the inhibitors: from bench to bedside. *Journal of hematology & oncology* 2013;**6**: 30.

5. Wu CP, Sim HM, Huang YH, Liu YC, Hsiao SH, Cheng HW, Li YQ, Ambudkar SV, Hsu SC. Overexpression of ATP-binding cassette transporter ABCG2 as a potential mechanism of acquired resistance to vemurafenib in BRAF(V600E) mutant cancer cells. *Biochem Pharmacol* 2013;**85**: 325-34.

6. Sun C, Wang L, Huang S, Heynen GJ, Prahallad A, Robert C, Haanen J, Blank C, Wesseling J, Willems SM, Zecchin D, Hobor S, et al. Reversible and adaptive resistance to BRAF(V600E) inhibition in melanoma. *Nature* 2014;**508**: 118-22.

7. Nakamura K, Okuyama R. Immunotherapy for advanced melanoma: Current knowledge and future directions. *Journal of dermatological science* 2016.

8. Bravo-Cordero JJ, Hodgson L, Condeelis J. Directed cell invasion and migration during metastasis. *Curr Opin Cell Biol* 2012;**24**: 277-83.

9. Chen YF, Chen YT, Chiu WT, Shen MR. Remodeling of calcium signaling in tumor progression. *J Biomed Sci* 2013;**20**: 23.

10. Roderick HL, Cook SJ. Ca2+ signalling checkpoints in cancer: remodelling Ca2+ for cancer cell proliferation and survival. *Nat Rev Cancer* 2008;**8**: 361-75.

11. Monteith GR, Davis FM, Roberts-Thomson SJ. Calcium channels and pumps in cancer: changes and consequences. *J Biol Chem* 2012;**287**: 31666-73.

12. Deli T, Varga N, Adam A, Kenessey I, Raso E, Puskas LG, Tovari J, Fodor J, Feher M, Szigeti GP, Csernoch L, Timar J. Functional genomics of calcium channels in human melanoma cells. *Int J Cancer* 2007;**121**: 55-65.

13. Stanisz H, Saul S, Muller CS, Kappl R, Niemeyer BA, Vogt T, Hoth M, Roesch A, Bogeski I. Inverse regulation of melanoma growth and migration by Orai1/STIM2-dependent calcium entry. *Pigment Cell Melanoma Res* 2014;**27**: 442-53.

14. Umemura M, Baljinnyam E, Feske S, De Lorenzo MS, Xie LH, Feng X, Oda K, Makino A, Fujita T, Yokoyama U, Iwatsubo M, Chen S, et al. Store-operated Ca2+ entry (SOCE) regulates melanoma proliferation and cell migration. *PLoS One* 2014;**9**: e89292.

15. Sun J, Lu F, He H, Shen J, Messina J, Mathew R, Wang D, Sarnaik AA, Chang WC, Kim M, Cheng H, Yang S. STIM1- and Orai1-mediated Ca(2+) oscillation orchestrates invadopodium formation and melanoma invasion. *J Cell Biol* 2014;**207**: 535-48.

16. Das A, Pushparaj C, Herreros J, Nager M, Vilella R, Portero M, Pamplona R, Matias-Guiu X, Marti RM, Canti C. T-type calcium channel blockers inhibit autophagy and promote apoptosis of malignant melanoma cells. *Pigment Cell Melanoma Res* 2013;**26**: 874-85.

17. Beck D, Niessner H, Smalley KS, Flaherty K, Paraiso KH, Busch C, Sinnberg T, Vasseur S, Iovanna JL, Driessen S, Stork B, Wesselborg S, et al. Vemurafenib potently induces endoplasmic reticulum stress-mediated apoptosis in BRAFV600E melanoma cells. *Sci Signal* 2013;**6**: ra7.

18. Curry MC, Roberts-Thomson SJ, Monteith GR. Plasma membrane calcium ATPases and cancer. *Biofactors* 2011;**37**: 132-8.

19. Strehler EE, Caride AJ, Filoteo AG, Xiong Y, Penniston JT, Enyedi A. Plasma membrane Ca2+ ATPases as dynamic regulators of cellular calcium handling. *Ann N Y Acad Sci* 2007;**1099**: 226-36.

20. Aung CS, Ye W, Plowman G, Peters AA, Monteith GR, Roberts-Thomson SJ. Plasma membrane calcium ATPase 4 and the remodeling of calcium homeostasis in human colon cancer cells. *Carcinogenesis* 2009;**30**: 1962-9.

21. Ribiczey P, Tordai A, Andrikovics H, Filoteo AG, Penniston JT, Enouf J, Enyedi A, Papp B, Kovacs T. Isoform-specific up-regulation of plasma membrane Ca2+ATPase expression during colon and gastric cancer cell differentiation. *Cell Calcium* 2007;**42**: 590-605.

22. Curry MC, Luk NA, Kenny PA, Roberts-Thomson SJ, Monteith GR. Distinct regulation of cytoplasmic calcium signals and cell death pathways by different plasma membrane calcium ATPase isoforms in MDA-MB-231 breast cancer cells. *J Biol Chem* 2012;**287**: 28598-608.

23. Varga K, Paszty K, Padanyi R, Hegedus L, Brouland JP, Papp B, Enyedi A. Histone deacetylase inhibitor- and PMA-induced upregulation of PMCA4b enhances Ca2+ clearance from MCF-7 breast cancer cells. *Cell Calcium* 2014;**55**: 78-92.

24. Ruschoff JH, Brandenburger T, Strehler EE, Filoteo AG, Heinmoller E, Aumuller G, Wilhelm B. Plasma membrane calcium ATPase expression in human colon multistep carcinogenesis. *Cancer Invest* 2012;**30**: 251-7.

25. Berger W, Elbling L, Minai-Pour M, Vetterlein M, Pirker R, Kokoschka EM, Micksche M. Intrinsic MDR-1 gene and P-glycoprotein expression in human melanoma cell lines. *Int J Cancer* 1994;**59**: 717-23.

26. Caride AJ, Filoteo AG, Enyedi A, Verma AK, Penniston JT. Detection of isoform 4 of the plasma membrane calcium pump in human tissues by using isoform-specific monoclonal antibodies. *Biochem J* 1996;**316 (Pt 1)**: 353-9.

27. Garay T, Juhasz E, Molnar E, Eisenbauer M, Czirok A, Dekan B, Laszlo V, Hoda MA, Dome B, Timar J, Klepetko W, Berger W, et al. Cell migration or cytokinesis and proliferation?--revisiting the "go or grow" hypothesis in cancer cells in vitro. *Exp Cell Res* 2013;**319**: 3094-103.

28. Hegedus B, Czirok A, Fazekas I, B'Abel T, Madar'asz E, Vicsek T. Locomotion and proliferation of glioblastoma cells in vitro: statistical evaluation of videomicroscopic observations. *J Neurosurg* 2000;**92**: 428-34.

29. Hegedus B, Zach J, Czirok A, Lovey J, Vicsek T. Irradiation and Taxol treatment result in non-monotonous, dose-dependent changes in the motility of glioblastoma cells. *J Neurooncol* 2004;**67**: 147-57.

30. Kolacsek O, Krizsik V, Schamberger A, Erdei Z, Apati A, Varady G, Mates L, Izsvak Z, Ivics Z, Sarkadi B, Orban TI. Reliable transgene-independent method for determining Sleeping Beauty transposon copy numbers. *Mob DNA* 2011;**2**: 5.

31. Chicka MC, Strehler EE. Alternative splicing of the first intracellular loop of plasma membrane Ca2+-ATPase isoform 2 alters its membrane targeting. *J Biol Chem* 2003;**278**: 18464-70.

32. Arbabian A, Brouland JP, Apati A, Paszty K, Hegedus L, Enyedi A, Chomienne C, Papp B. Modulation of endoplasmic reticulum calcium pump expression during lung cancer cell differentiation. *FEBS J* 2013;**280**: 5408-18.

33. Grusch M, Schelch K, Riedler R, Reichhart E, Differ C, Berger W, Ingles-Prieto A, Janovjak H. Spatio-temporally precise activation of engineered receptor tyrosine kinases by light. *EMBO J* 2014;**33**: 1713-26.

34. Hummel D, Aggarwal A, Borka K, Bajna E, Kallay E, Horvath HC. The vitamin D system is deregulated in pancreatic diseases. *J Steroid Biochem Mol Biol* 2014;**144 Pt B**: 402-9.

35. Garbe C, Abusaif S, Eigentler TK. Vemurafenib. *Recent Results Cancer Res* 2014;**201**: 215-25.

36. Wimmer R, Baccarini M. Partner exchange: protein-protein interactions in the Raf pathway. *Trends Biochem Sci* 2010;**35**: 660-8.

37. Akinleye A, Furqan M, Mukhi N, Ravella P, Liu D. MEK and the inhibitors: from bench to bedside. *J Hematol Oncol* 2013;**6**: 27.

38. Paszty K, Caride AJ, Bajzer Z, Offord CP, Padanyi R, Hegedus L, Varga K, Strehler EE, Enyedi A. Plasma membrane Ca2+-ATPases can shape the pattern of Ca2+ transients induced by store-operated Ca2+ entry. *Sci Signal* 2015;**8**: ra19.

39. Maurer G, Tarkowski B, Baccarini M. Raf kinases in cancer-roles and therapeutic opportunities. *Oncogene* 2011;**30**: 3477-88.

40. Klein RM, Spofford LS, Abel EV, Ortiz A, Aplin AE. B-RAF regulation of Rnd3 participates in actin cytoskeletal and focal adhesion organization. *Mol Biol Cell* 2008;**19**: 498-508.

41. Makrodouli E, Oikonomou E, Koc M, Andera L, Sasazuki T, Shirasawa S, Pintzas A. BRAF and RAS oncogenes regulate Rho GTPase pathways to mediate migration and invasion properties in human colon cancer cells: a comparative study. *Mol Cancer* 2011;**10**: 118.

42. Nieto MA. Epithelial plasticity: a common theme in embryonic and cancer cells. *Science* 2013;**342**: 1234850.

43. Rhodes DR, Yu J, Shanker K, Deshpande N, Varambally R, Ghosh D, Barrette T, Pandey A, Chinnaiyan AM. ONCOMINE: a cancer microarray database and integrated data-mining platform. *Neoplasia* 2004;**6**: 1-6.

44. Haqq C, Nosrati M, Sudilovsky D, Crothers J, Khodabakhsh D, Pulliam BL, Federman S, Miller JR, 3rd, Allen RE, Singer MI, Leong SP, Ljung BM, et al. The gene expression signatures of melanoma progression. *Proceedings of the National Academy of Sciences of the United States of America* 2005;**102**: 6092-7.

45. Talantov D, Mazumder A, Yu JX, Briggs T, Jiang Y, Backus J, Atkins D, Wang Y. Novel genes associated with malignant melanoma but not benign melanocytic lesions. *Clinical cancer research : an official journal of the American Association for Cancer Research* 2005;**11**: 7234-42.

46. Rinker-Schaeffer CW, O'Keefe JP, Welch DR, Theodorescu D. Metastasis suppressor proteins: discovery, molecular mechanisms, and clinical application. *Clin Cancer Res* 2006;**12**: 3882-9.

47. Hurst DR, Welch DR. Metastasis suppressor genes at the interface between the environment and tumor cell growth. *Int Rev Cell Mol Biol* 2011;**286**: 107-80.

48. Yang S, Zhang JJ, Huang XY. Orai1 and STIM1 are critical for breast tumor cell migration and metastasis. *Cancer Cell* 2009;**15**: 124-34.

49. Potier M, Gonzalez JC, Motiani RK, Abdullaev IF, Bisaillon JM, Singer HA, Trebak M. Evidence for STIM1- and Orai1-dependent store-operated calcium influx through ICRAC in vascular smooth muscle cells: role in proliferation and migration. *FASEB J* 2009;**23**: 2425-37.

50. Stanisz H, Saul S, Muller CS, Kappl R, Niemeyer BA, Vogt T, Hoth M, Roesch A, Bogeski I. Inverse regulation of melanoma growth and migration by Orai1/STIM2-dependent calcium entry. *Pigment Cell Melanoma Res*;**27**: 442-53.

51. Umemura M, Baljinnyam E, Feske S, De Lorenzo MS, Xie LH, Feng X, Oda K, Makino A, Fujita T, Yokoyama U, Iwatsubo M, Chen S, et al. Store-operated Ca2+ entry (SOCE) regulates melanoma proliferation and cell migration. *PLoS One*;**9**: e89292.

52. Arozarena I, Sanchez-Laorden B, Packer L, Hidalgo-Carcedo C, Hayward R, Viros A, Sahai E, Marais R. Oncogenic BRAF induces melanoma cell invasion by downregulating the cGMP-specific phosphodiesterase PDE5A. *Cancer Cell* 2011;**19**: 45-57.

53. Tsai FC, Seki A, Yang HW, Hayer A, Carrasco S, Malmersjo S, Meyer T. A polarized Ca2+, diacylglycerol and STIM1 signalling system regulates directed cell migration. *Nat Cell Biol* 2014;**16**: 133-44.

54. Baggott RR, Alfranca A, Lopez-Maderuelo D, Mohamed TM, Escolano A, Oller J, Ornes BC, Kurusamy S, Rowther FB, Brown JE, Oceandy D, Cartwright EJ, et al. Plasma membrane calcium ATPase isoform 4 inhibits vascular endothelial growth factor-mediated angiogenesis through interaction with calcineurin. *Arterioscler Thromb Vasc Biol* 2014;**34**: 2310-20.

Figure legends

Figure 1. PMCA4b is upregulated in BRAF mutant melanoma cells after inhibition of the BRAF-MEK-ERK pathway

 (A1) Two BRAF wild type (MEWO, MJZJ) and two BRAF mutant (A375, A2058,) cell lines were treated with mutant BRAF inhibitor vemurafenib (V; 0.5 µM, 72 h) or GDC0879 (G; 0.5 µM, 72 h), and the protein level of PMCA4b, PMCA1, pERK1,2 and ERK1,2 proteins were analyzed by Western Blotting of total cell lysates (20 µg per sample). (A2) Densitometric analysis of the Western Blots. Changes in PMCA4b protein level were expressed as fold increase over the untreated controls. (B1) Change of PMCA4b, SERCA2 and SERCA3 proteins in the BRAF mutant A375 cell line upon treatments with the indicated amounts of vemurafenib for 72 hours. (B2) Concentration dependent change of PMCA4b protein in the BRAF mutant A375, A2058 and the BRAF wild type MEWO cell lines. Changes in PMCA4b protein level were expressed as fold increase over the untreated controls. Bars represent means ± SE from three to five independent experiments. Based on these results, 0.5 µM vemurafenib concentration was chosen for further experiments.(C1) BRAF mutant (A375, A2058), BRAF wild-type but NRAS mutant (MJZJ) and BRAF and NRAS wild-type (MEWO) cell lines were treated with MEK inhibitor selumetinib (0.5 µM) for 72 hours. (C2) Densitometric analyses of PMCA4b levels of total cell lysates (20µg per sample). Data are expressed as fold increase over the untreated controls. Bars represent means ± SE from two to three independent experiments.

Figure 2. Enhanced abundance of PMCA4b in BRAF mutant cells is associated with an enhanced Ca^{2+} clearance. (A) Immunofluorescence staining of BRAF mutant (A375, A2058) and BRAF and NRAS wild-type (MEWO) melanoma cells. Cells were treated with 0.5 µM vemurafenib for 72 hours, then immunostaining was performed with anti-PMCA4b antibody

(JA3). Images were taken by confocal microscopy with 60X magnification. (B, C1) Ca^{2+} signaling measurement in vemurafenib-treated (0.5µM, 48hours) melanoma cells. Intracellular Ca^{2+} level was detected by Fluo-4 Ca^{2+} indicator. After Ca^{2+} - store depletion by thapsigargin (Tg) and ATP, a transient increase in intracellular Ca^{2+} was generated by allowing Ca^{2+} entry through the store operated Ca^{2+} channels (SOCs). Data represent fluorescent intensity values (F/F0) of 10-30 cells and are representative of three independent determinations. (D1, 2) Intracellular Ca^{2+} signal was initiated by the Ca^{2+} ionophore A23187 in control and vemurafenib-treated A375 cells. External media was changed to HBSS supplemented with 2 mM Ca^{2+} and 2µM A23187 was added as indicated. Treatment with Lanthanum (1mM, $LaCl_3$) was applied when peak intensity was reached. Data represent fluorescent intensity values of 10-15 cells. (C2, D3) Half peak decay time of the second phase of the transients (SOCE) and of the A23187 induced transient in control and vemurafenib-treated A375 cells were determined. Bar graphs are mean ± SD of individual cells taken from two to three independent experiments. Significances between control and vemurafenib-treated cells are denoted by *** ($P<0.001$); two-tailed unpaired t-test.

Figure 3. Vemurafenib inhibits the migration of BRAF mutant melanoma cells. Migration of BRAF wild type (MEWO) and BRAF mutant (A2058, A375) cell lines was followed by time-lapse video microscopy for 72 hours in the presence or absence of vemurafenib (0.5 µM). (A) Single cell migration trajectories of untreated A375 *(left graph)* and vemurafenib-treated A375 *(right graph)* between 48-72 hours. Plots show migration trajectories of 20 -24 cells with the starting position of each trajectory translated to the origin of the plot. (B) Net displacement was determined between 0-12 and 48-60 hours. Data shown is mean +/- SEM of at least four independent measurements. ** ($P<0.01$), ** ($P<0.01$); two tailed Student's t-test.

Figure 4. Generation of PMCA4b expressing cell lines. Wild type BRAF (MEWO) and mutant BRAF (A375) cells were stably transfected with GFP or GFP-tagged PMCA4b. (A) A375-GFP4b-I and A375-GFP4b-II cell lines were generated independently from each other. (B) GFP-PMCA4b localized mainly in the plasma membrane. Images were taken by confocal microscope with 60X magnification. Scale bar, 20 μm. (C) Cell proliferation was analyzed by measuring BrdU incorporation. Data shown is the mean +/- SEM of three independent measurements. Asterisks denote significant differences between vemurafenib treated versus untreated cells (*: P<0.05; **: P<0.01, two tailed Student's t-test).

Figure 5. PMCA4b overexpression decreased the migratory activity of BRAF mutant A375 cells. (A) The migratory activity of A375-GFP, A375-GFP-PMCA4b-I, A375-GFP-PMCA4b-II, MEWO-GFP and MEWO-GFP-PMCA4b cells was analyzed by time-lapse video microscopy for 16 hours, as described above. (A1) shows single cell migration trajectories of A375-GFP (left graph) and A375-GFP-PMCA4b (right graph). Plots show migration trajectories of 25 -30 cells with the starting position of each trajectory translated to the origin of the plot. (A2) Net displacement of cells was evaluated for 12 hours of migration. Data shown is mean +/- SEM of at least four independent measurements. Significances between control and vemurafenib-treated cells are denoted by ** (P<0.01) *** (P<0.001); two-tailed unpaired t-test. (B) Cell-shape analysis of the A375-GFP and A375-GFP-PMCA4b cells. (B1) Images show contours of GFP- and GFP-PMCA4b-expressing A375 cells. (B2) Area, circularity and aspect of ratio ((major axis) / (minor axis)) parameters of A375 cells expressing GFP (n = 249) or GFP-PMCA4b (n = 204) were compared. Bars represent means ± SEM from 3 independent experiments. Asterisks (***) denote significant differences compared to cells expressing GFP (p<0.0001, two-tailed unpaired t-test).

Figure 6. PMCA4b overexpression decreased the metastatic potential of BRAF mutant A375 cells. For in vivo colony formations assays, 4×10^4 cells / mouse (n=10) were injected into the tail-vein and mice were sacrificed after 6 weeks. (A) The number of animals with lung metastasis was significantly reduced in groups injected with PMCA4b overexpressing A375 cells as compared with controls (Chi-square test, P=0.034) (B) The graph shows the total area of tumors in each group after the analysis of hematoxylin-stained tissue sections. (C) Representative images of hematoxylin-eosin sections from mice injected with A375-GFP, A375-GFP-PMCA4b-I or A375-GFP-PMCA4-II cells. White and black asterisks indicate tumors growing in the lung parenchyma and in the associated connective tissue, respectively. Black arrows indicate tumor cell invasion along vessels and bronchiole. Black arrowheads show tumors growing in the interlobular space.

Figure 1.
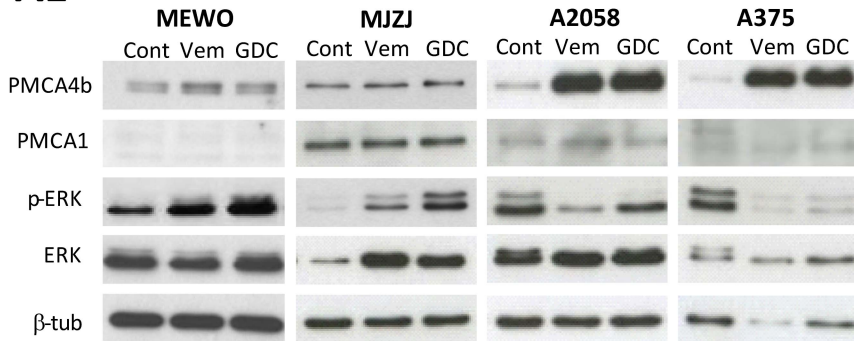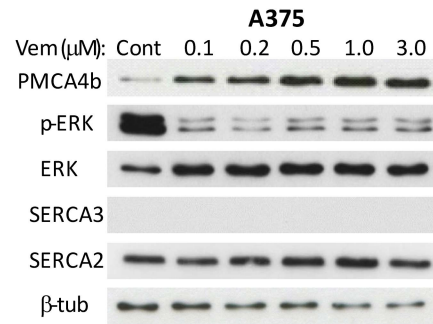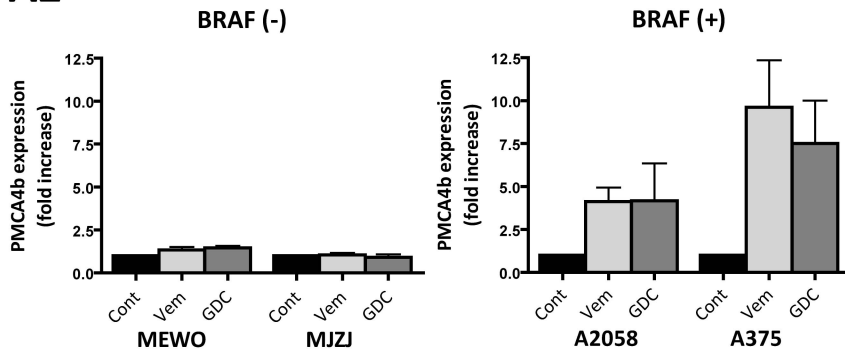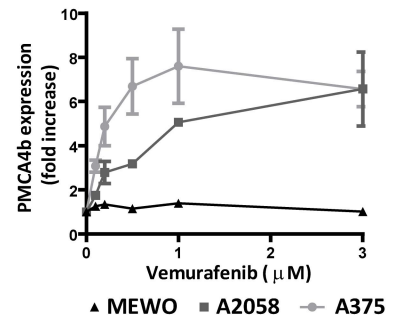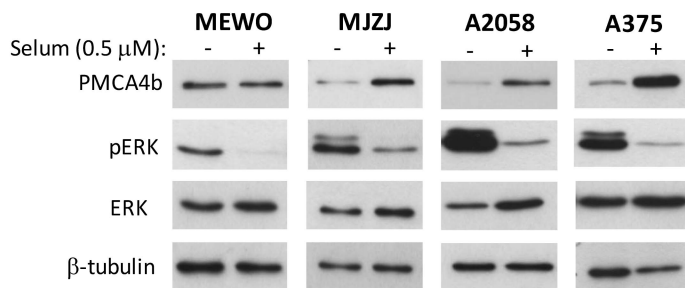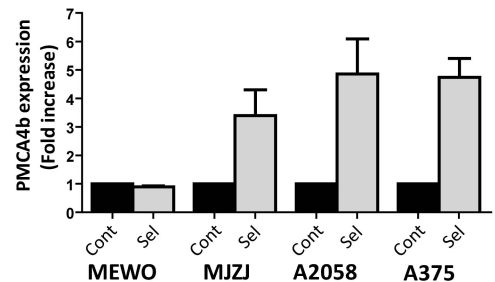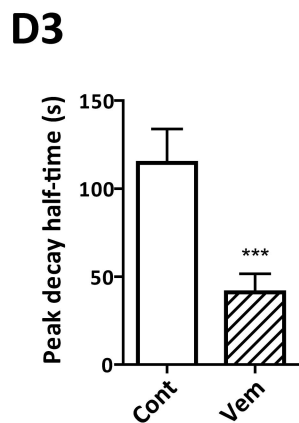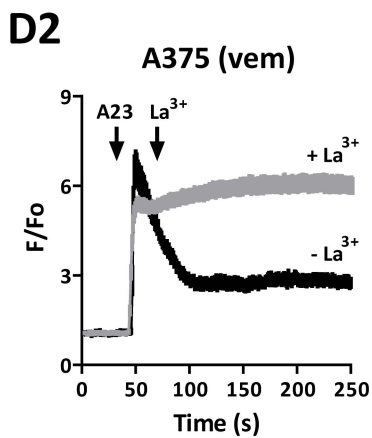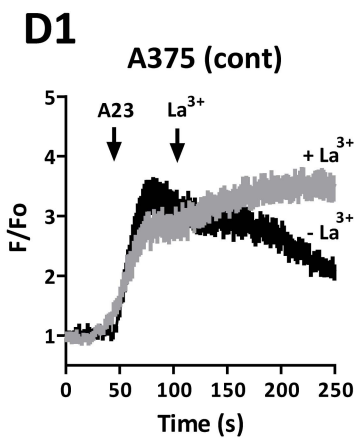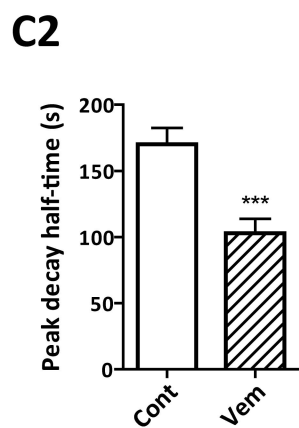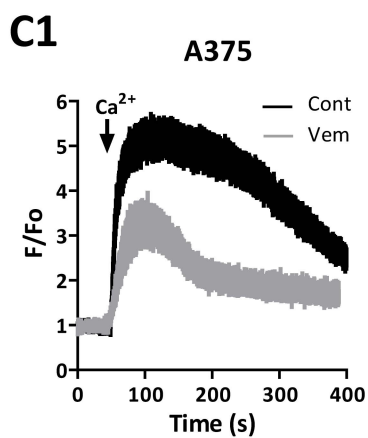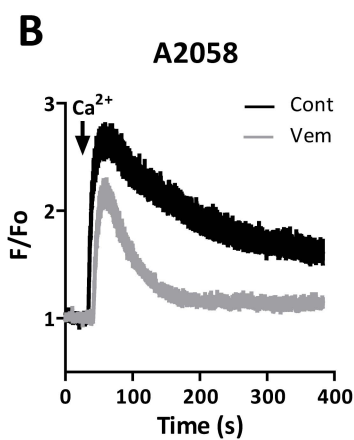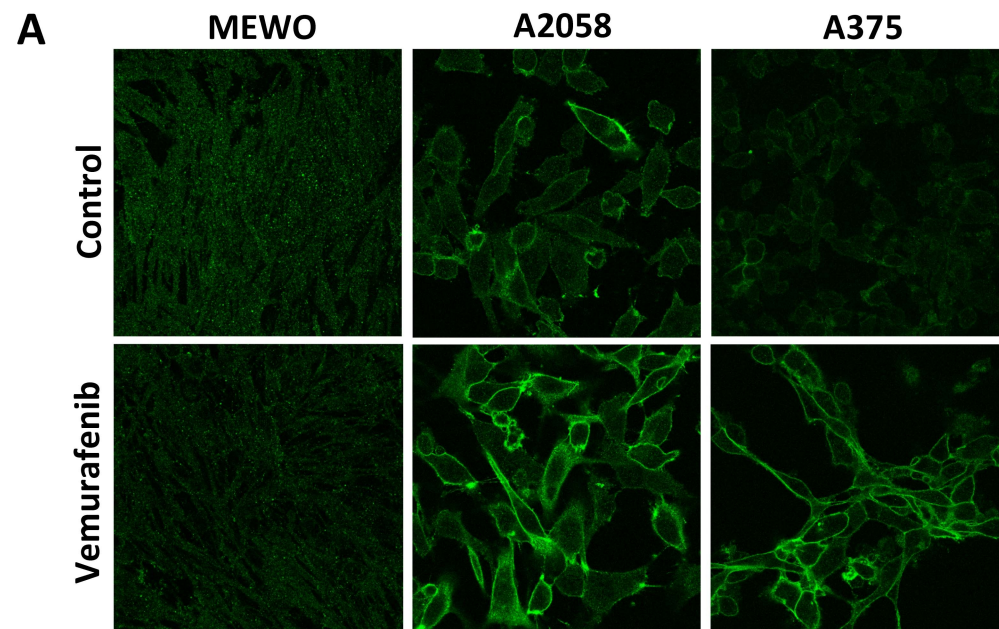
Figure 2.

A

	MEWO	A2058	A375
Control			
Vemurafenib			

B A2058

C1 A375

C2

D1 A375 (cont)

D2 A375 (vem)

D3

Figure 3.

Figure 4

A

MEWO   A375

GFP | GFP4b | GFP | GFP4bI. | GFP4bII.

— GFP-PMCA4b
— PMCA4b

— BRAFV600E

— pERK

B

A375-GFP | A375-GFP4b

MEWO-GFP | MEWO-GFP4b

C

BrdU incorporation (fold change)

** ** * *

A375 cont | A375 vem | GFP cont | GFP vem | 4bI cont | 4bI vem | 4bII cont | 4bII vem

Figure 5

Figure 6

A

B

C

A375-GFP   **A375-PMCA4b-II**

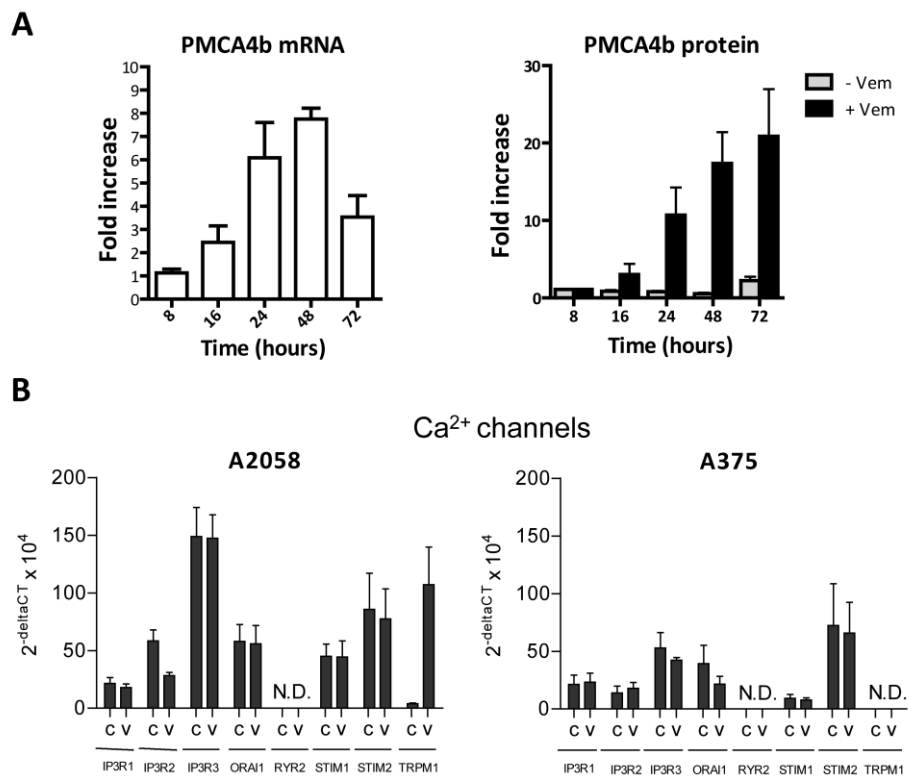150 µm   150 µm
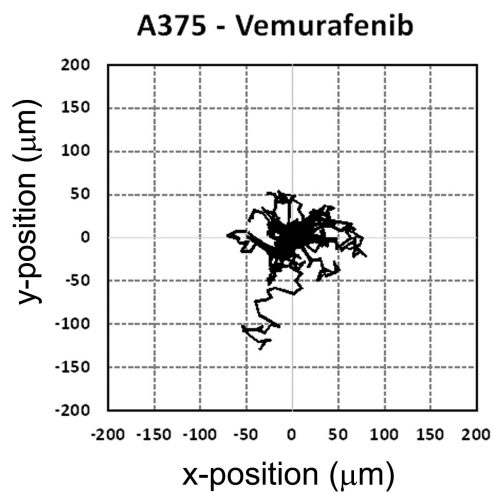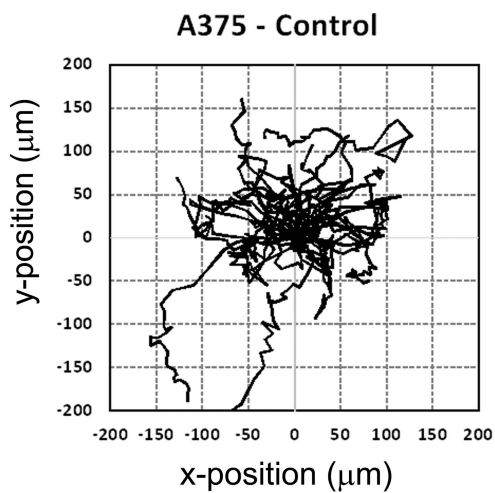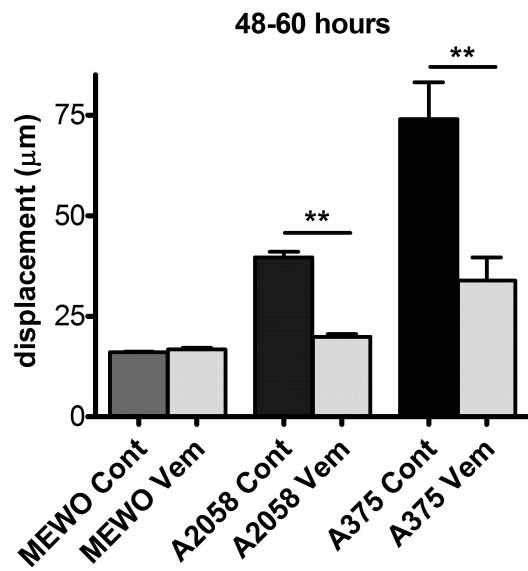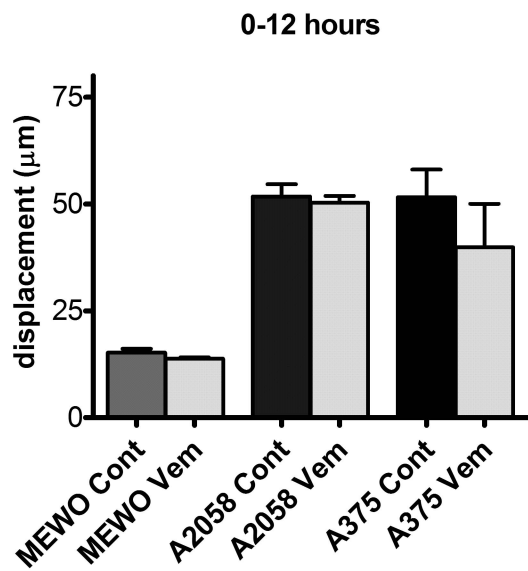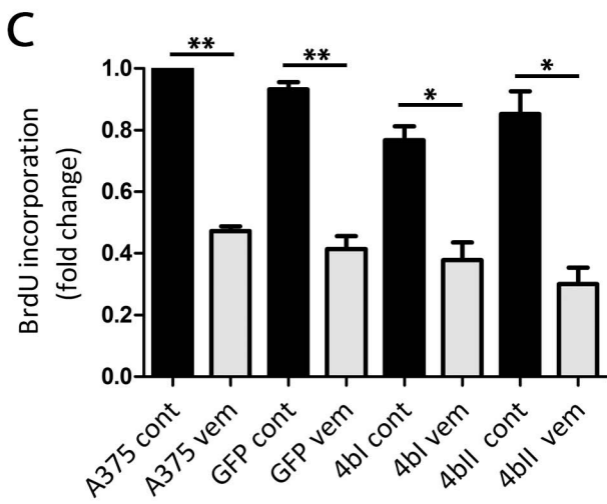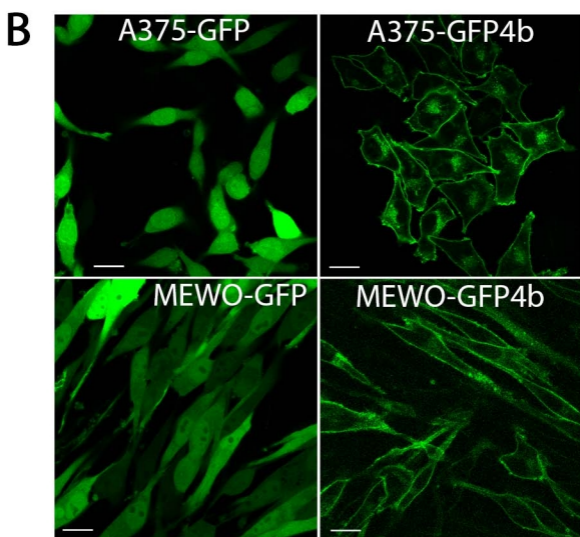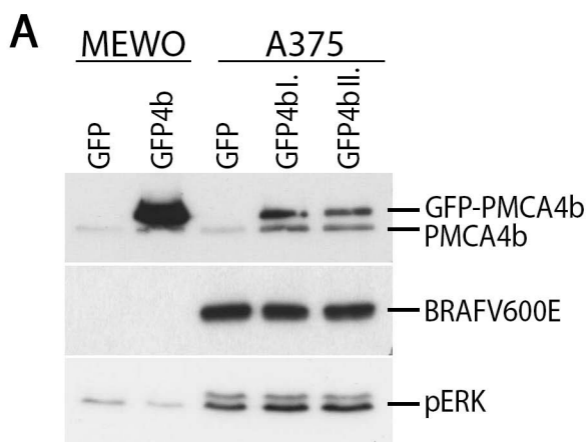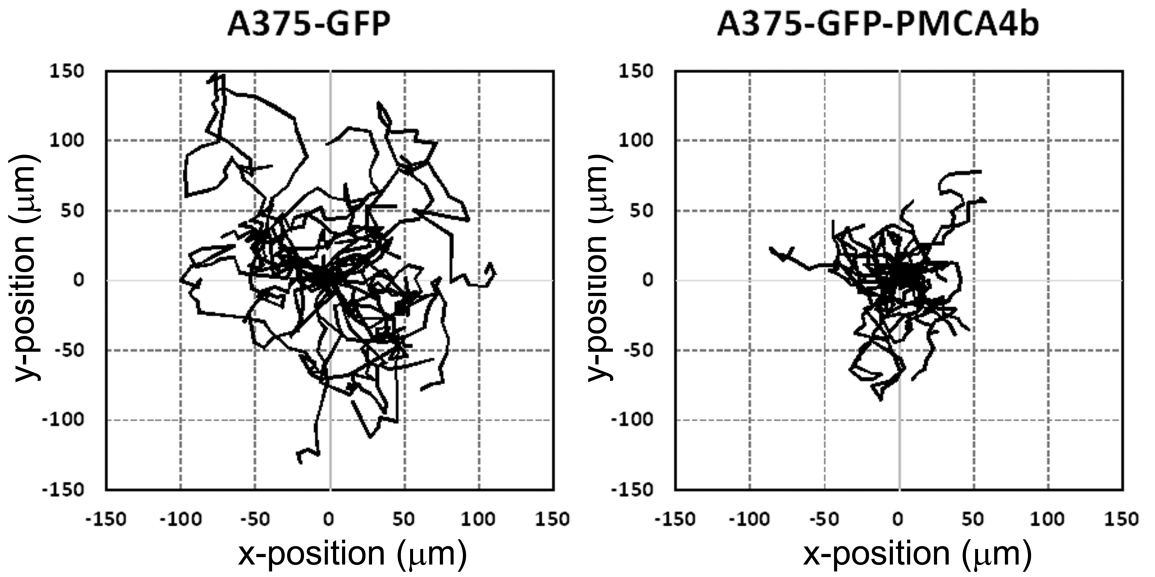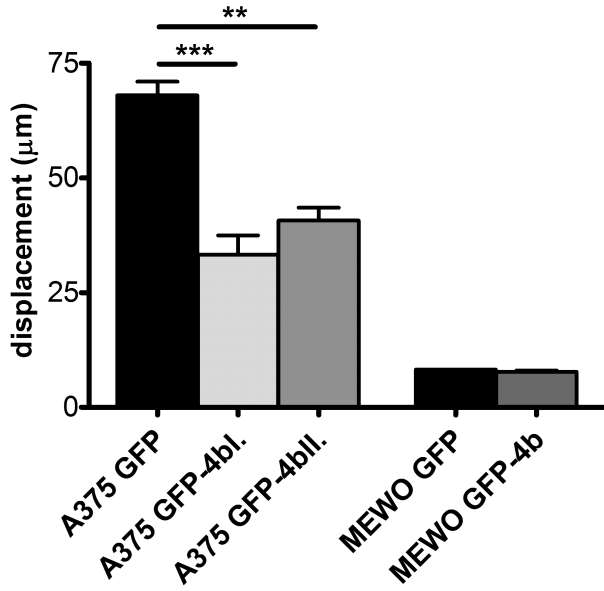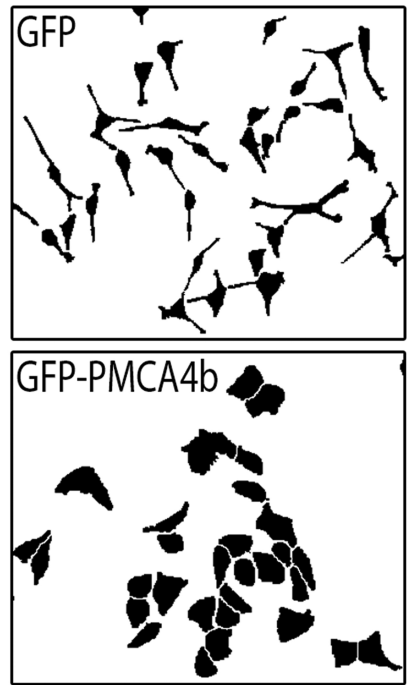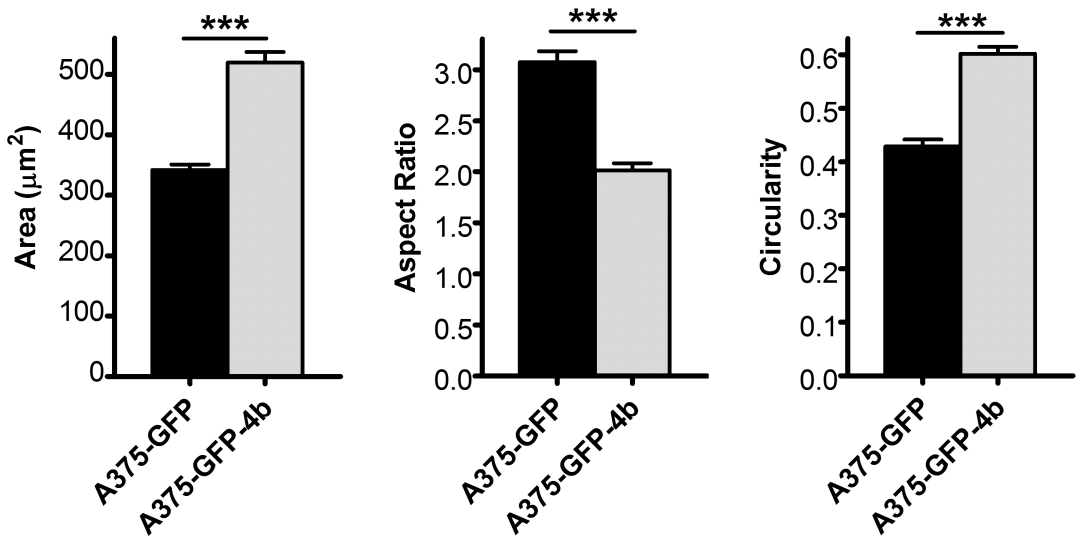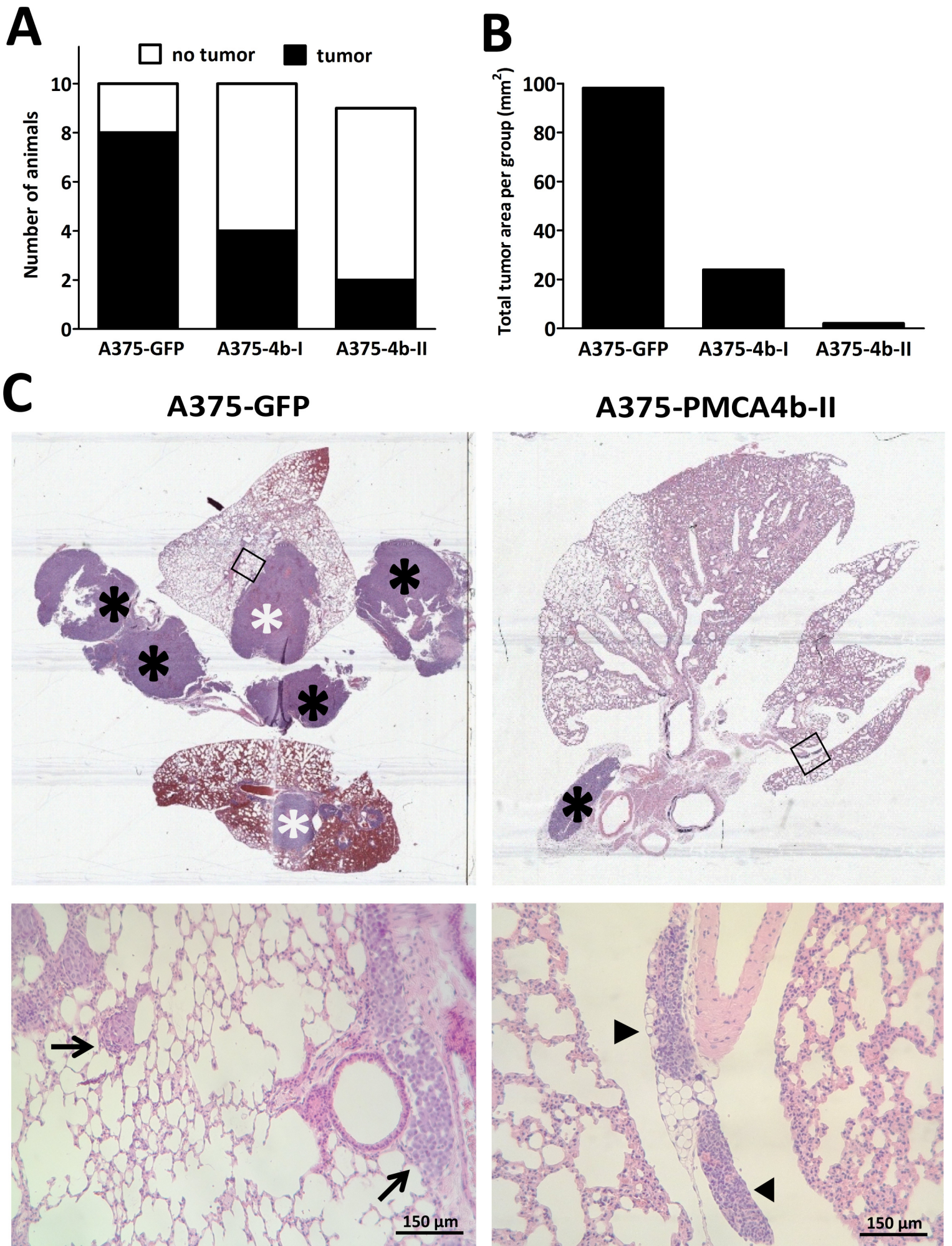
Figure S1. Effect of vemurafenib on mRNA expression of Ca^{2+} channels and PMCA4b in A375 cells. (A) Expression of PMCA4b was analyzed at mRNA and protein levels after 0.5μM vemurafenib treatment at the indicated time points by quantitative real-time PCR and Western Blot analysis, respectively. (B) A2058 and A375 cells were treated with 0.5 μM of the mutant BRAF inhibitor vemurafenib (V) or solvent as control (C) for 48 h. Expression of inositol 1,4,5-triphosphate receptor type 1-3 (IP3R1, IP3R2, IP3R3), ORAI calcium release-activated calcium modulator 1 (ORAI1), ryanodine receptor 2 (RYR2), stromal interaction molecule 1 and 2 (STIM1, STIM2), transient receptor potential cation channel subfamily M member 1 (TRPM1was analyzed by quantitative real-time PCR analysis. Expression was normalized to glyceraldehyde-3-phosphate dehydrogenase (GAPDH) and bars represent means and SEM of two independent experiments performed in duplicates. N.D., not detectable.
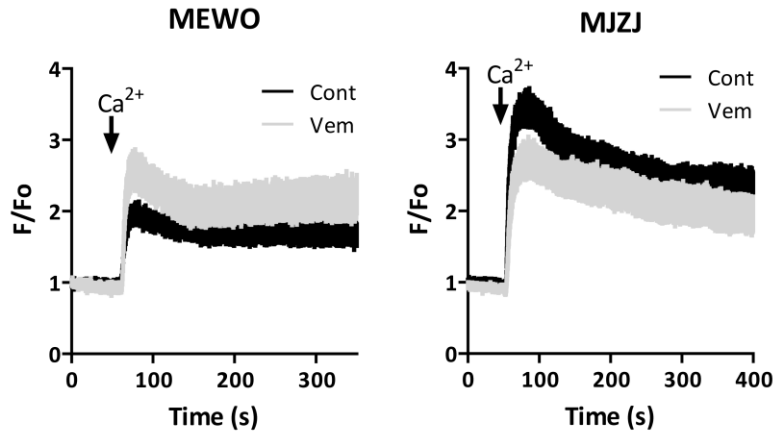
Figure S2. Ca^{2+} signaling measurement in control or 0.5 µM vemurafenib treated (48 hours) non-BRAF mutant melanoma cell lines MZJZ and MEWO. Measurement was performed as described in figure 2.
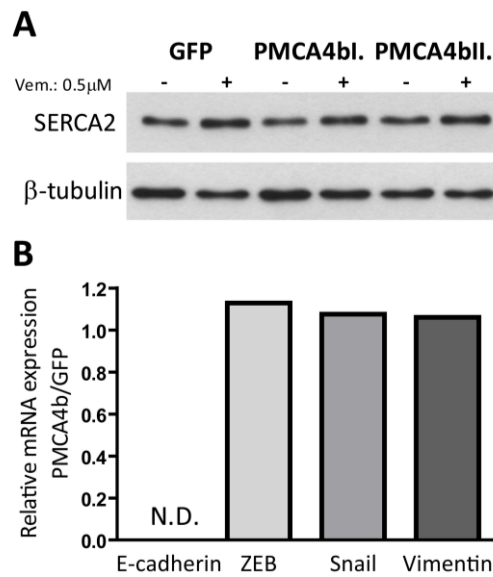

Figure S3. (A) Expression of SERCA2 in vemurafenib treated and control GFP and GFP-PMCA4b expressing cell lines. (B) EMT marker proteins (E-cadherin, ZEB-1, Snail and vimentin) were compared between A375-GFP and A375-GFP-PMCA4b cells by quantitative real-time PCR analysis. N.D., not detectable.
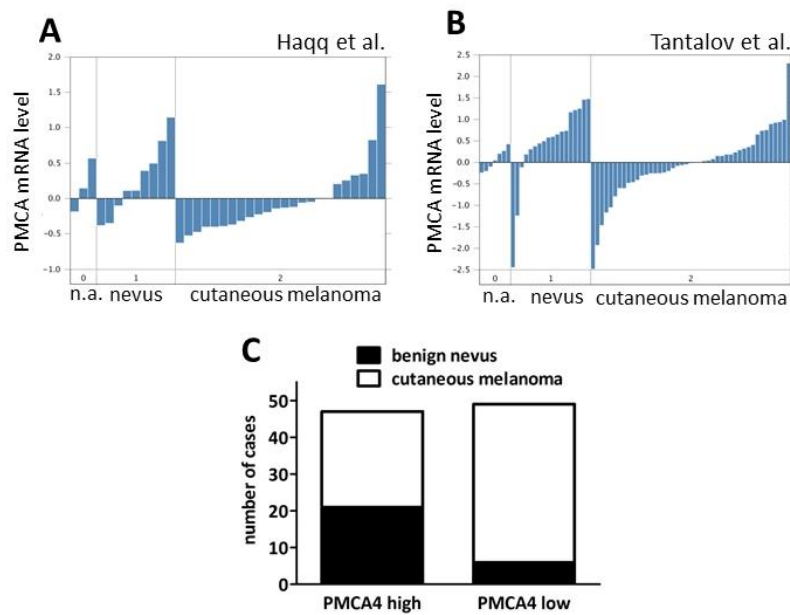
Figure S4. Gene expression microarray data analysis for PMCA4b expression. (A,B)

Using the ONCOMINE platform, cutaneous melanoma samples showed a decreased

PMCA4b expression when compared to benign nevi in two gene expression microarray

dataset where direct comparison was possible. (C) After pooling the data from the two cohorts

there was a significantly higher number of cases with low PMCA4b expression in the

cutaneous melanoma group (p= 0.0006).

Supplementary movies:

Supplementary Movie S1. Three-day long time-lapse videomicroscopy measurement of
A375-GFP- cells. Most cells display an elongated shape with pronounced extensions and
demonstrate very high migratory activity.

Supplementary Movie S2. Three-day long time-lapse videomicroscopy measurement of
A375-GFP-PMCA4b cells. Note the altered morphology of the cells and the profound
decrease in migratory activity as compared to Supplementary Movie S1.

Supplementary table S1:

Primers used for SYBR Green expression analysis

Oligo Name	Sequence (5'-3')
IP3R1 forward	TTG GGC CTG GTT GAT GAT CG
IP3R1 reverse	TTT GGG CAG AGT AGC GGT TC
IP3R2 forward	AGA AGA ATG CCA TGC GTG TG
IP3R2 reverse	ACC CTC GCT TCT CAG TTT CC
IP3R3 forward	CCT AAG AAG TTC CGT GAC TG
IP3R3 reverse	TCC TTG TCC TGC TTA GTC TG
ORAI1 forward	TGG ACG CTG ACC ACG ACT AC
ORAI1 reverse	CCT CGA TGT TGG GCA GGA TG
RYR2 forward	ATG TAT CTG TGC TGC CTG TC
RYR2 reverse	CTT CTG ATC GCT GCT TAG AG
STIM1 forward	GAT GGA CGA TGA TGC CAA TG
STIM1 reverse	GAA GGT GCT GTG TTT CAC TG
STIM2 forward	AAC GAC ACT TCC CAG GAT AG
STIM2 reverse	ACC ACA TCC AAT GCC TTG AG
TRPM1 forward	GTG TCA GCA CAG GTG TTA TC
TRPM1 reverse	TCC TTT CCA ACC AGG TCT TC